

Two-dimensional electron-gas mobility in GaAs/Al_xGa_{1-x}As: Deformation-potential study including hydrostatic-pressure effects

I. Gorczyca

Unipress, Polish Academy of Sciences, Sokolowska 29, PL 01-142 Warsaw, Poland

J. Krupski

*Institute of Theoretical Physics, Warsaw University, Hoza 69, PL 00-681 Warsaw, Poland
and the Institute of Physics, Bialystok Branch of Warsaw University, Lipowa 41, PL 15-424 Bialystok, Poland
(Received 29 March 1994; revised manuscript received 24 October 1994)*

The mobility of a two-dimensional (2D) electron gas in two different samples of a GaAs/Al_xGa_{1-x}As heterostructure is calculated as a function of temperature, electron concentration, and hydrostatic pressure and compared with previously published experimental data. It follows from our discussion that, compared to the Thomas-Fermi method, the random-phase approximation describes the screening of the scattering potentials much better. Separation of the acoustic phonon scattering from other scattering mechanisms allows the determination of the conduction-band deformation potential constant E_D . The resulting deformation potential is found to be -12.0 ± 1.0 eV, which is in agreement with the most frequently reported data for GaAs/Al_xGa_{1-x}As heterostructures. The hydrostatic-pressure dependence of the deformation potential is also studied (using the heterostructure with higher electron mobility) and, contrary to the common assumptions about the pressure independence of E_D , we have found that its absolute value decreases with applied hydrostatic pressure. Polar optical phonon scattering is also considered, including the screening by a 2D electron gas.

I. INTRODUCTION

Two-dimensional electron systems in semiconductors have an increasing importance for application in solid state electronics (high-speed logical circuits, laser diodes, etc.). The interest in the electronic properties of a two-dimensional electron gas (2DEG) confined at the interface of the GaAs/Al_xGa_{1-x}As heterostructure is motivated by the large enhancement of the electron mobility compared to three-dimensional semiconductors. Mobility enhancement in the GaAs/Al_xGa_{1-x}As heterostructure represents one of the major goals of semiconductor technology.

An immediate improvement is associated with the introduction of the concept of modulation-doped heterostructures (MDH) for a GaAs/Al_xGa_{1-x}As system. This is because the 2DEG confined at the GaAs side of the interface is separated by an undoped spacer from parent donors which are in Al_xGa_{1-x}As.^{1,2} This causes a large reduction of ionized impurity scattering, which is usually the dominant scattering mechanism limiting the electron mobility at low temperatures. The enhancement of electron mobility in MDH now approaches four orders of magnitude.³ Further progress can be achieved by improvement of epitaxy conditions and optimization of the MDH structures, which requires a detailed study of the physical processes limiting the mobility. The aim of our paper is an investigation of the scattering mechanisms limiting the mobility of the 2DEG in modulation-doped GaAs/Al_xGa_{1-x}As heterostructures.

To understand the importance of the various scatter-

ing mechanisms in a 2D system a systematic study of mobility as a function of different parameters, especially of the electron concentration, should be made. However, it is difficult to compare theory and experiment from such a study, since by nature practically each heterojunction is unique. In this situation hydrostatic pressure experiments are a very useful tool for 2D electron transport effect investigations, as they allow the electronic properties of the heterojunction to be precisely modified without changing the intrinsic properties of the material. The high-pressure freezeout (HPFO) method, combined with the persistent photoconductivity (PPC) effect inducing changes of electron concentration in a given sample, gives an important advantage in comparison with the usual situation where a set of samples is employed.⁴⁻⁷

The HPFO method has seldom been employed in this kind of study whereas the PPC effect has become very popular. The former method makes it possible to decrease drastically the concentration of the 2DEG. In contrast, the latter procedure is used to increase the density of the 2DEG.

For the purpose of this work we employ experimental results published elsewhere.⁸⁻¹⁰ However, to enable the reader to achieve a full understanding of the problems considered, we will include a short description of the examined samples as well as the high-pressure methods used in the experiments.

The measurements we consider were carried out on two different samples: a GaAs/Al_{0.35}Ga_{0.65}As heterostructure with conventional bulk doping of the barrier (sample A) and a GaAs/Al_{0.3}Ga_{0.7}As heterostructure with a

δ -doped barrier (sample *B*).

First (sample *A*), the electron mobility as a function of temperature and the 2DEG concentration, $n_{2\text{DEG}}$, was studied. Owing to the use of the HPFO method and PPC it became possible to obtain different electron concentrations using one sample of the considered heterostructure only.

Next, the pressure dependence of electron mobility, concentrating on the deformation potential behavior, was examined. To this aim the higher-mobility sample (sample *B*) was used.

In our theoretical analysis we put the main emphasis on two disputable problems: (1) What is the magnitude of the deformation potential E_D , and a related question—whether E_D originating from acoustic phonons should be screened or not? (2) Does E_D depend on pressure? The third problem we want to consider is changes in the mobility due to polar optical phonon scattering including the screening by 2DEG. Some of the results were published elsewhere.^{8–10}

The conduction-band E_D value determined in various bulk GaAs materials ranges mainly from -7 to -9.5 eV (e.g., Refs. 11 and 12). More recent studies of acoustic phonon scattering (APS) in GaAs/ $\text{Al}_x\text{Ga}_{1-x}\text{As}$ 2DEG structures gave E_D values ranging between -8 and -16 eV.^{13–21} The values of E_D we obtained for two different samples and for various 2DEG concentrations vary between -11.5 and -12.5 eV.

Discussing different models for screening by 2DEG we prove that, contrary to some suggestions,^{18,19} the deformation potential has to be screened by free carriers. It turns out that the Thomas-Fermi method is unable to describe the screening effects properly, so in order to achieve an agreement between theory and experiment we use the random-phase approximation (RPA) to account for this phenomenon.

In Sec. II the details of samples and experiments we discussed are given; in Sec. III the method of calculations is outlined, and the results are presented in Sec. IV. Discussion and comparison with other experimental and theoretical results together with some conclusions are in Sec. V.

II. SAMPLES

To investigate the temperature dependencies of mobility for different values of 2DEG concentration $n_{2\text{DEG}}$, the sample with high electron concentration $n_{2\text{DEG}} = 2.6 \times 10^{11} \text{ cm}^{-2}$ and electron mobility at 4.2 K equal to $\mu = 4.7 \times 10^5 \text{ cm}^2/\text{V s}$ was chosen (sample *A*). This sample was characterized by the possibility of changing the $n_{2\text{DEG}}$ values in a wide range due to the HPFO procedure (decreasing of $n_{2\text{DEG}}$), and using the PPC effect (increasing of $n_{2\text{DEG}}$). The sample was grown by molecular beam epitaxy.^{8,9} It was a GaAs/ $\text{Al}_{0.35}\text{Ga}_{0.65}\text{As}$ heterostructure consisting of Si-doped $\text{Al}_x\text{Ga}_{1-x}\text{As}$, an undoped $\text{Al}_x\text{Ga}_{1-x}\text{As}$ spacer, and undoped GaAs grown on a semi-insulating GaAs substrate [see Fig. 1(a) for the detailed scheme]. The HPFO procedure consists of applying pressure at room temperature, which leads to the capture of carriers by localized Si-donor states in $\text{Al}_x\text{Ga}_{1-x}\text{As}$. Releasing pressure at $T < 100$ K does not change the occupancy of donors, and one can thus produce an arbitrary change of $n_{2\text{DEG}}$, which persists at ambient pressure. The higher the value of pressure applied at high temperatures, the lower the magnitude of $n_{2\text{DEG}}$. At low temperatures an increase of $n_{2\text{DEG}}$ may be induced after shining a light on the sample. This effect (PPC) persists after the light is turned off, if the temperature does not exceed 100 K. The measurements of Hall concentration and mobility were performed at atmospheric pressure.

The mobility of the sample described above was too low for a precise determination of the pressure effects, so that the sample with a much higher value of μ was chosen (sample *B*) to investigate the temperature dependence of μ , with hydrostatic pressure as a parameter. The high electron mobility enables us to easily extract the APS mechanism, which is dominant under these conditions. However, the technique of growing high-mobility samples leads to low electron concentration. In view of the fact that the optimum condition for our study was a high electron concentration–high mobility (as will be explained in more detail in Sec. IV), the PPC procedure was used to get a maximum 2DEG concentration.^{8–10} The resulting

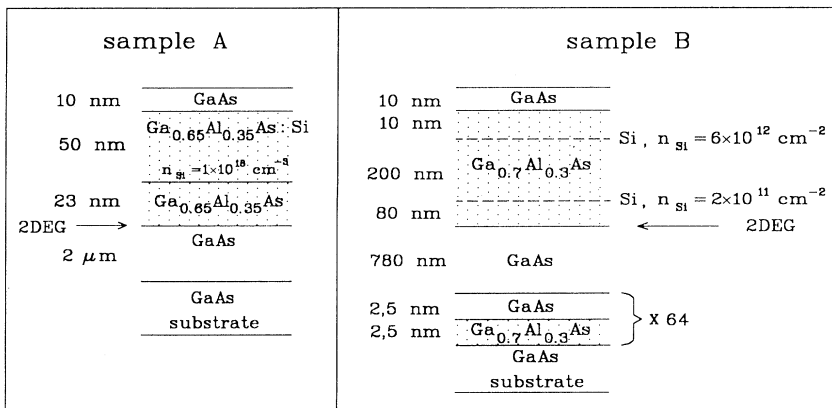


FIG. 1. Structures of the samples used in this study.

$n_{2\text{DEG}}$ for sample *B* was $1.9 \times 10^{11} \text{ cm}^{-2}$. The sample was prepared by molecular beam epitaxy with the implementation of the doping in the $\text{Al}_{0.3}\text{Ga}_{0.7}\text{As}$ using two δ -doped layers of Si.¹⁰ They are separated by a large spacer to create a structure with high electron mobility by removing the scattering due to the potential fluctuations associated with the surface space charge.²² A scheme of the sample is given in Fig. 1(b). The described growth procedure leads to a large reduction of ionized impurity scattering, thus the obtained 2DEG Hall mobility μ was as high as $2.7 \times 10^6 \text{ cm}^2/\text{V s}$ (at atmospheric pressure and $T = 4.2 \text{ K}$). The employed experimental data consist of results of the measurements of $n_{2\text{DEG}}$ and μ as a function of temperature between 4.2 and 70 K and for four different hydrostatic-pressure values (0, 0.53, 0.8, and 1.1 GPa). All the results were obtained in the dark, after illumination of the sample (at 30 K) by a red-light-emitting diode in order to get the maximum concentration $n_{2\text{DEG}}$ at every value of the used pressure (PPC). In this situation $n_{2\text{DEG}}$ shows a very weak dependence on temperature. A decrease of $n_{2\text{DEG}}$ with pressure—about 40% for 1 GPa—is observed.

III. THEORY

The temperature dependence of the electron mobility is evaluated theoretically in the temperature range 4.2–70 K, and 2DEG density range $0.5\text{--}5 \times 10^{11} \text{ cm}^{-2}$, and for four values of hydrostatic pressure: 0, 0.53, 0.80, and 1.1 GPa. To calculate the mobility we solve the Boltzmann equation in the relaxation time approximation. In our study we take into account all relevant scattering mechanisms that limit the mobility: (1) Ionized impurity scattering (IIS) corresponding to (i) background residual impurities in GaAs, (ii) impurities from the undoped spacer layer of $\text{Al}_x\text{Ga}_{1-x}\text{As}$, (iii) ionized Si donors from the $\text{Al}_x\text{Ga}_{1-x}\text{As}$ barrier, (iv) compensated acceptors in $\text{Al}_x\text{Ga}_{1-x}\text{As}$. (2) Acoustic phonon scattering (deformation potential and piezoelectric scattering). (3) Polar optical phonon scattering.

We neglect here contributions given by the interface roughness and the alloy-disorder scattering. As it was shown in Ref. 23, these two mechanisms can be effective in determining the mobility in GaAs/ $\text{Al}_x\text{Ga}_{1-x}\text{As}$ at electron concentrations $n_{2\text{DEG}}$ higher than 10^{12} cm^{-2} . Moreover, the alloy-disorder scattering can play a role at small Al content x only ($x \approx 0.1$).²³ Note that in our case the highest $n_{2\text{DEG}}$ is $4.6 \times 10^{11} \text{ cm}^{-2}$ and $x = 0.35$ for sample *A* and 0.30 for sample *B*.

With decreasing temperature, below about 70 K, the major mechanism limiting the 2DEG mobility changes from optical phonon scattering (OPS) to acoustic phonon scattering (APS). The APS contribution, composed of the deformation-potential scattering and piezoelectric scattering of the 2DEG, decreases with lowering temperature, and ionized impurity scattering becomes the dominant mechanism.

The electron mobility (averaged over energy) is given by (see, for example, Ref. 24, Sec. IV.3)

$$\mu = \frac{\int_0^\infty \mu(E) E (-df_0/dE) dE}{\int_0^\infty E (-df_0/dE) dE} \quad (1)$$

with

$$\frac{1}{\mu(E)} = \frac{m}{e} \sum_p \frac{1}{\pi} \int_0^\pi \frac{\nu_p}{\epsilon^2(q)} (1 - \cos \varphi) d\varphi + \frac{1}{\mu_{\text{opt}}(E)}, \quad (2)$$

where E_0 is the energy of the subband bottom, and $q = \frac{2}{\hbar} (2m|E - E_0|)^{1/2} \sin \frac{\varphi}{2}$.

The ν_p value depends on the particular scattering mechanism ($\nu_{\text{ion}}, \nu_{\text{def}}, \nu_{\text{piezo}}$), and on the form of wave function we assume. For example, if the electron density is²⁵ (ϑ is the Heaviside step function)

$$\rho(z) = \vartheta(z) \left(\frac{1}{2}\right)^3 b z^2 \exp(-bz), \quad (3)$$

we have

$$\nu_{\text{ion}} = 4\pi^2 \frac{m e^4}{\hbar^3} \frac{1}{q^2} \iint n(z) \rho(z') e^{-q|z'-z|} dz dz', \quad (4a)$$

where $n(z)$ is the 2D ionized impurity concentration,

$$\nu_{\text{def}} = \frac{3mk_B T E_D^2}{16\hbar^3 C_l} \quad (4b)$$

(C_l is the longitudinal elastic constant).

The piezoelectric contribution consists of two parts, longitudinal and transverse:

$$\nu_{\text{piez}} = \nu_{\text{piezL}} + 2\nu_{\text{piezT}}. \quad (5)$$

They are²⁶

$$\nu_{\text{piezL}} = \frac{m}{\hbar^3} (eh_{14})^2 \frac{k_B T}{2\kappa_L} \frac{9}{32} f_L(q), \quad (5a)$$

$$\nu_{\text{piezT}} = \frac{m}{\hbar^3} (eh_{14})^2 \frac{k_B T}{2\kappa_T} \frac{13}{32} f_T(q). \quad (5b)$$

Here κ_L and κ_T are the longitudinal and transverse elastic constants, respectively, and h_{14} is the appropriate piezoelectric tensor component (see Table I). Functions f_L and f_T are

$$f_{L,T} = \iint \rho(z_1) \rho(z_2) \exp(-q|z_1 - z_2|) \times \gamma_{L,T}(q|z_1 - z_2|) dz_1 dz_2 \quad (5c)$$

with $\gamma_{L,T}$ given by

$$\gamma_L(u) = (1/3) (3 + 3u - u^3) \exp(-u), \quad (5d)$$

$$\gamma_T(u) = (1/13) (13 + 13u - 14u^2 + 3u^3) \exp(-u). \quad (5e)$$

Usually when deriving ν_{def} the Bose-Einstein distribution for phonons, i.e., $N = [\exp(\hbar\omega/k_B T) - 1]^{-1}$, is ap-

TABLE I. Parameters determined and employed in the present calculations.

		Sample A	Sample B
Carrier concentration (cm ⁻³)	N_b	8×10^{17}	5×10^{17}
	N_{sp}	1×10^{15}	1×10^{14}
	N_D	3×10^{14}	1×10^{14}
Effective mass	m	0.067 m_0	
Dielectric constants	ϵ_0	12.7	
	ϵ_∞	10.8	
Elastic constants	c_{11}	11.8×10^{11} dyn/cm ²	
	c_{12}	5.32×10^{11} dyn/cm ²	
Piezoelectric coupling parameter	h_{14}	1.45×10^7 V/cm	

proximated by $K_B T / \hbar \omega$ not only at high temperatures, where these should be nearly the same, but for all T values. This leads to the formula (4b) and finally causes some error in ν_{def} which is shown in Fig. 5(b). To avoid this error in our calculations we used the actual form of the Bose-Einstein distribution function in the very-low-temperature region and therefore ν_{def} in this region can only be determined numerically.

To calculate the relaxation time it is necessary to take into account a screening of the scattering potentials. A frequently occurring situation is that where the screened potential (i.e., the potential experienced by electrons) differs only slightly from the bare or external potential. In such a case the relation between the screened (V_{eff}) and the external (V_{ext}) potentials can be expressed by a dielectric function:

$$V_{\text{eff}}(q) = V_{\text{ext}}(q) / \epsilon(q). \quad (6)$$

In the approach where the screening by 2DEG is ignored the dielectric function reduces to a constant, i.e., $\epsilon(q) = \epsilon_0$. A simple way of including the 2DEG contribution consists of replacing ϵ_0 by the Thomas-Fermi (TF) expression, which turns out to be the small- q limit of the more accurate formula for the dielectric function obtained within the random-phase approximation. Recently, while analyzing experimental data, several authors^{8,9,21} came to the conclusion that, in contrast to the RPA, both the Thomas-Fermi approach and that with screening by ϵ_0 are not satisfactory in the case of 2DEG in GaAs/Al_xGa_{1-x}As heterostructures. It is worthwhile to mention that the importance of the corrections introduced by the RPA method as compared with the Thomas-Fermi theory was already emphasized²⁷ and confirmed²⁸ in the case of silicon inversion layers.

The RPA dielectric function for 2DEG at $T = 0$ K is of the form (see, for example, Ref. 24)

$$\epsilon(q, T, E_F) = \epsilon_0 + \frac{2\pi e^2}{q} F(q) \Pi(q, T, E_F), \quad (7)$$

where

$$F(q) = \iint \rho(z) \exp(-q|z - z'|) \rho(z') dz dz' \quad (8)$$

and²⁹

$$\Pi(q, T, E_F) = \frac{\int_0^\infty dE' \Pi(q, T = 0, E')}{4k_B T \cosh^2[(E - E_F) / 2k_B T]} \quad (9)$$

with³⁰

$$\Pi(q, T = 0, E') = \frac{m}{\pi \hbar^2} \{1 - \vartheta(q - 2k) [1 - (2k/q)^2]^{1/2}\}, \quad (10)$$

where

$$k' = (2m |E' - E_0|)^{1/2} / \hbar. \quad (11)$$

As can be seen from the above, the dielectric function at finite temperature is obtained from the expression for $T = 0$ by simple numerical integration.²⁹

For the unscreened case (without screening by 2DEG, i.e., $\Pi = 0$) the dielectric function reduces to the dielectric constant of the medium surrounding the 2DEG, i.e., $\epsilon(q, T, E_F) = \epsilon_0$. In the case of Thomas-Fermi screening (small- q limit of RPA dielectric function):

$$\Pi(q, T = 0, E) = \frac{m}{\pi \hbar^2} \quad (12)$$

and

$$\Pi(q, T, E_F) = \frac{m}{2\pi \hbar^2} [1 + \tanh(E_F / 2k_B T)]. \quad (13)$$

Note that the acoustic phonon scattering involves phonons with low energies, which means that it can be treated as an elastic process ($\hbar \omega \rightarrow 0$). Consequently, considering the screening, we ignored, as it is commonly treated, the dependence of the dielectric function.

The theoretical evaluation of the mobility faces difficulties due to the uncertainty of IIS, which includes contributions from different regions of the heterostructure. The general situation for a modulation-doped heterostructure is schematically presented in Fig. 2, where the ionized impurity profile of a "bulk-doped" heterostructure is shown for two values of hydrostatic pressure [Figs. 2(a) and 2(b)]. The GaAs layer (b) is nominally undoped and contains only background residual impurities N_b , while the mixed Al_xGa_{1-x}As crystal is selectively doped, i.e., it contains the undoped region—spacer (s) with a very

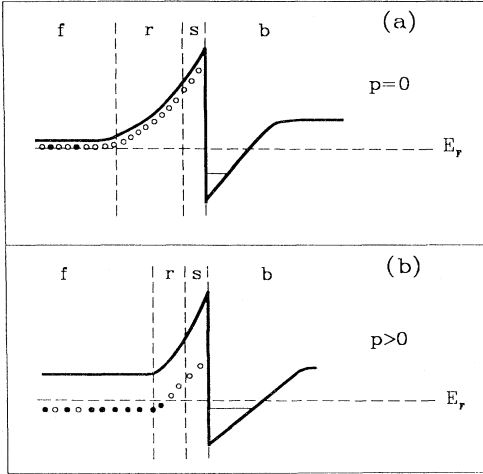


FIG. 2. The conduction-band diagram for modulation-doped heterojunction. (a) Ambient pressure case; (b) with hydrostatic pressure applied. Different regions are denoted as follows. *b*: nominally undoped GaAs; *s*: undoped $\text{Al}_x\text{Ga}_{1-x}\text{As}$ layer (spacer); *r*: doped $\text{Al}_x\text{Ga}_{1-x}\text{As}$ layer with the donor impurities located high above the Fermi level; *f*: the rest of the doped $\text{Al}_x\text{Ga}_{1-x}\text{As}$ layer.

small ionized impurity concentration N_{sp} —and the region highly doped with Si. The latter consists of two parts: The first part is the depleted region (*r*) with the ionized impurity concentration $N_r = N_A + N_D$, N_A being the concentration of compensated acceptors (the $\text{Al}_x\text{Ga}_{1-x}\text{As}$ material is assumed to be partially compensated) and N_D being the concentration of ionized donors (as a result of the electron affinity difference between GaAs and $\text{Al}_x\text{Ga}_{1-x}\text{As}$ materials, the electrons from the donors in the doped $\text{Al}_x\text{Ga}_{1-x}\text{As}$ layer are transferred to GaAs). The second part (*f*) has the concentration of ionized impurities $N_F = 2N_A$, and contains also the neutral Si donors. The width L of the depletion region is determined from the neutrality condition

$$(N_D - N_A)L = n_{2\text{DEG}} + n_{\text{depl}}, \quad (14)$$

where n_{depl} is the 2DEG ionized impurity concentration in the depleted region of GaAs.

The application of hydrostatic pressure causes a downward shift of the DX centers. When they are below the bottom of the conduction band the deionization of Si donor states takes place. The free electron concentration $n_{2\text{DEG}}$ in the quantum well decreases and, as a consequence [as is seen from (9)], the width of the depletion region, L , decreases. This situation is illustrated in Fig. 2(b). Decreasing the temperature causes a nonequilibrium metastable freezeout of electrons on impurities sites, and the charge distribution remains the same while releasing pressure.

In the case of a δ -doped heterostructure all the impurities that give electrons to the 2DEG are at the same distance from the heterostructure, and now the parameter

dependent on pressure is the amount of ionized impurities in the δ -layer, instead of the width L of the depletion region.

In principle, the momentum relaxation time does not exist for polar optical phonon scattering, which is an inelastic process. However, in the very special cases, e.g., $kT \ll \hbar\omega_{\text{LO}}$, such a relaxation time can be introduced to a good approximation. To determine μ_{opt} we derived the two-dimensional version of the formula proposed in Ref. 31 for the three-dimensional case. Assuming that the phonons are not influenced by the layered structure and using the Fröhlich Hamiltonian, we get

$$\frac{1}{\mu_{\text{opt}}(E)} = \frac{Nme}{8\pi\hbar\epsilon^*k} \frac{k_{\text{LO}}^2}{(k^2 + k_{\text{LO}}^2)} \left[4I_1 - \frac{(k_{\text{LO}}^2 I_0 - I_1)^2}{k^2 I_0} \right], \quad (15)$$

where $k = [2m(E - E_0)]^{1/2}/\hbar$, $k_{\text{LO}} = (2m\hbar\omega_{\text{LO}})^{1/2}/\hbar$, and $\epsilon^* = (1/\epsilon_\infty - 1/\epsilon_0)^{-1}$ (ϵ_∞ and ϵ_0 are optical and static dielectric constants, respectively),

$$I_i = \int_{q_{\text{min}}}^{q_{\text{max}}} dq_\perp \frac{q_\perp^i u(q_\perp)}{\left[1 - \left(\frac{q_\perp^2 - k_{\text{LO}}^2}{2kq_\perp} \right)^2 \right]^{1/2}} \quad (i = 0, 1) \quad (16)$$

and $q_{\text{min}} = (k_{\text{LO}}^2 + k^2)^{1/2} - k$, $q_{\text{max}} = (k_{\text{LO}}^2 + k^2)^{1/2} + k$. Function u depends on the form of the electron density ρ ,

$$u(q_\perp) = \frac{1}{|\epsilon(q_\perp, \omega_{\text{LO}}, T)|^2} \times \int dq_z \frac{1}{q_z^2 + q_\perp^2} \left| \int dz \rho(z) e^{iq_z z} \right|^2 \quad (17)$$

and for ρ given by (3) can be calculated analytically. The frequency-dependent dielectric function takes here the form

$$\epsilon(q_\perp, \omega, T) = 1 + \frac{2\pi e^2}{\epsilon_\infty q_\perp} F(q_\perp) \Pi(q_\perp, \omega, T, E_F), \quad (18)$$

where $F(q_\perp)$ is given by (8) and the temperature-dependent polarization part, $\Pi(q, \omega, T, E)$, can be calculated according to (9) with $\Pi(q, \omega, T = 0, E)$ given in Refs. 24, 30, and 32. Note that $\text{Im}\Pi = 0$ when $\omega = 0$ and the polarization part reduces to (10).

So far μ_{opt} for polar optical phonon scattering was calculated by ignoring the screening by 2DEG and taking either the scattering rate instead of the momentum relaxation time or by assuming the validity of the relaxation time approximation in a wide range of temperatures.^{33–36} The importance of the screening of scattering potential due to the polar optical phonons was emphasized already in Ref. 37. The dynamic screening of the interaction of the electrons with the polar optical phonons was extensively discussed in papers by Ridley and co-workers,^{38,39} where it was pointed out that for higher carrier densities the screening becomes of considerable importance and its dynamic nature must be taken into account. In previous

papers⁸⁻¹⁰ we used a three-dimensional approach to polar optical phonon scattering (see, for example, Ref. 40).

Since our purpose is to study the deformation-potential behavior, we will concentrate on the APS mechanism. However, the procedure of extracting APS from the measured low-temperature mobility data requires a precise determination of the IIS contribution. Thus, the distribution of ionized impurities in the 2D channel of GaAs and in the doped as well as undoped (spacer) region of $\text{Al}_x\text{Ga}_{1-x}\text{As}$ have to be determined unequivocally. For this purpose, in the absence of directly measured values of the charge concentration in all three regions, we had to fit our calculations to the existing μ against $n_{2\text{DEG}}$ experimental data at lowest temperatures. Details of this procedure will be described in Sec. IV.

IV. RESULTS

A. Mobility versus temperature. Determination of the deformation-potential constant

We start by discussing the results obtained for sample A, i.e., calculated and experimental mobility as a function of temperature for different values of $n_{2\text{DEG}}$. At equilibrium conditions the 2DEG concentration was found to be $2.6 \times 10^{11} \text{ cm}^{-2}$. The HPFO method gave the following set of $n_{2\text{DEG}}$: 2.03, 1.73, 1.04, $0.55 \times 10^{11} \text{ cm}^{-2}$, while using the PPC effect made it possible to get the two highest ones: 3.63 and $4.60 \times 10^{11} \text{ cm}^{-2}$. Thus, the procedures used allowed seven different values of electron concentration to be obtained in one sample. For the purpose of the performed analysis we limited the experimental data to the five highest concentrations. We rejected the two lowest ones from our detailed study for the following reasons.

(1) For small $n_{2\text{DEG}}/n_{\text{depl}}$ ratios the variational wave function we use²⁵ may not be sufficiently accurate (see Ref. 21 and references therein).

(2) Analyzing different scattering mechanisms which limit the electron mobility, one can see that the main contribution in the case of low values of $n_{2\text{DEG}}$ comes from IIS, whereas other scattering mechanisms are much weaker in the whole considered range of temperature. The calculated electron mobility against temperature is shown in Fig. 3 for an electron concentration $n_{2\text{DEG}} = 0.55 \times 10^{11} \text{ cm}^{-2}$. Contributions corresponding to different scattering mechanisms are drawn separately. A determination of the IIS contribution can give pronounced errors due to the uncertainty of the charge distribution in various layers of the heterostructure, so a much more convenient situation from our point of view is the case in which the IIS contribution is small, and APS is dominant.

The role of the particular scattering mechanisms will be discussed in the intermediate case of $n_{2\text{DEG}} = 2.6 \times 10^{11} \text{ cm}^{-2}$, as an example. In Fig. 4 the calculated electron mobility versus temperature with contributions corresponding to different scattering mechanisms is presented for the considered electron concentration. Below 70 K APS is the dominant mechanism limiting the

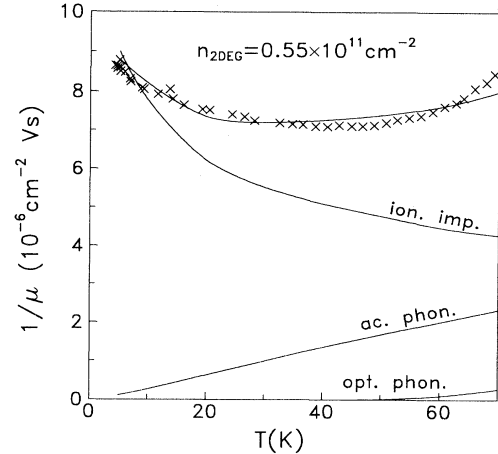


FIG. 3. Reciprocal mobility versus temperature for 2DEG concentration $n_{2\text{DEG}} = 0.55 \times 10^{11} \text{ cm}^{-2}$ (sample A). Various theoretical curves correspond to the different scattering mechanisms: ionized impurities, acoustic phonons, and optical phonons. The upper curve corresponds to the total mobility according to the rule $1/\mu_{\text{Tot}} = 1/\mu_{\text{ion}} + 1/\mu_{\text{ac}} + 1/\mu_{\text{opt}}$. Experimental points are indicated by crosses.

2DEG mobility. The contribution from optical phonons is smaller and negligible below 40 K. IIS is dominant at low temperatures. One can see from the decomposition in Fig. 4 that it is easy in our case to separate contributions from different scattering mechanisms: IIS causes almost a uniform vertical displacement of the total mobility curve, OPS causes the nonlinearity over 40 K, and the change of the APS contribution due to the different possible values of the deformation potential influences the slope of the total mobility curve.

As was already mentioned in Sec. III, the main difficulty in the theoretical evaluation of the mobility consists of an uncertainty of the IIS contribution. This results

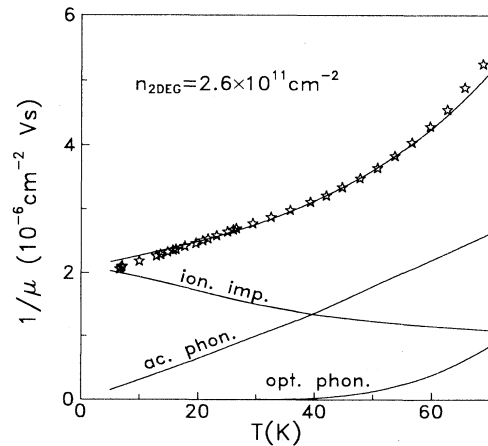


FIG. 4. The same as Fig. 3, but for $n_{2\text{DEG}} = 2.6 \times 10^{11} \text{ cm}^{-2}$.

from the lack of knowledge of the exact charge distribution in various layers of the heterostructure. Fortunately, due to the fact that IIS gives in our case a small contribution to the total scattering, the rough data on the charge distribution (obtained during the growth process) and a fit of the calculated mobility to the experimental results at the lowest temperatures permitted us to determine the IIS in the whole temperature region. Our procedure is the following.

(1) First we try to fit the calculated electron mobility at lowest temperature to the experimental curves for different $n_{2\text{DEG}}$, treating charge distributions as fitting parameters—the input values are N_b , N_{sp} , and N_D , known approximately from the growth procedure. The results are independent of E_D , because it influences only the slope of the curve, but not its value at the lowest temperature.

(2) Next, having the IIS contribution, we fit the electron mobility in the whole temperature range, treating E_D as a parameter.

(3) Additionally, trying to get the best fit (simulating the total mobility) above 40 K, we can establish the OPS contribution. The resulting frequency of the longitudinal optical phonons, involved in this scattering process, is 33.5 eV, which is in good agreement with the values reported in the literature⁴¹ (32–36 eV).

The same procedure can also be applied to the calculations based on data describing sample *B*. Here, in contrast to the first case, we focus our attention on the pressure dependence of mobility, keeping $n_{2\text{DEG}}$ constant. The established charge distributions for both heterostructures together with other parameters and constants used in our calculation are given in Table I.

Calculated and experimental electron mobilities for sample *A* are presented in Fig. 5, where the temperature dependence of $1/\mu$ for various $n_{2\text{DEG}}$ is shown. In Fig. 5(a) the results obtained using the original Bose-Einstein distribution function to derive ν_{def} are presented. In Fig. 5(b) the comparison of these results with those obtained from the approximate formula for the distribution function (see Sec. III) is given.

Fitting the experimental curves μ versus T for different values of $n_{2\text{DEG}}$, we can find the value of E_D . In the first approach, we assumed, in accordance to the suggestion in Ref. 18, that E_D was not screened by the 2DEG. This leads to the result shown in Fig. 6 by crosses. Considerable changes of the deformation potential constant E_D with $n_{2\text{DEG}}$ showed that the used assumption is unlikely. A significant decrease of E_D with increasing 2DEG concentration strongly suggests the importance of screening. Thus in the next step of our analysis we took into account the effect of screening employing (i) the temperature-dependent Thomas-Fermi dielectric function and (ii) the dielectric function obtained within the framework of the random-phase approximation.^{24,30,32} The E_D values versus $n_{2\text{DEG}}$ obtained within model (ii) gave E_D much more stable, relative to the other two fits, in the whole range of $n_{2\text{DEG}}$ (see Fig. 6) and equal to 12.0 ± 0.5 eV. As can be seen in Fig. 6, model (i) leads to less satisfactory results. Assuming that the value of E_D is between -12.5 and -11.5 eV, one can see that the Thomas-Fermi method,

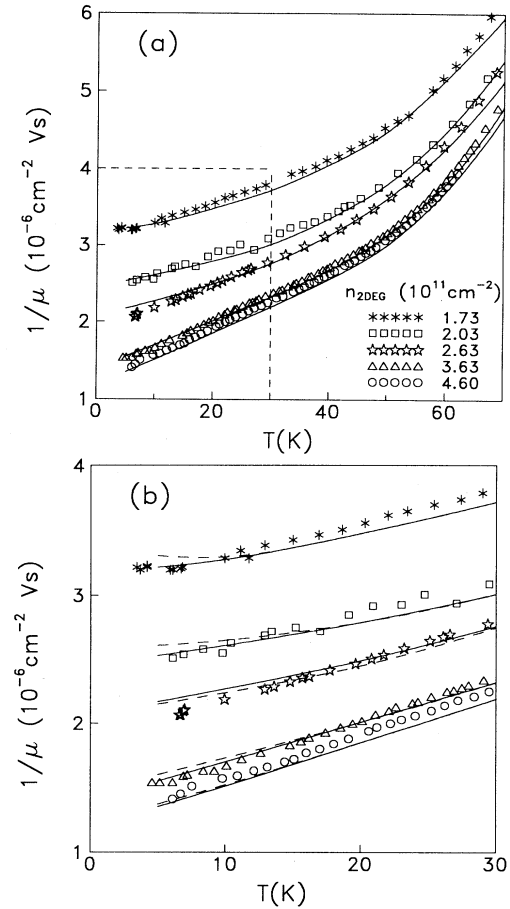


FIG. 5. The temperature dependence of reciprocal mobility for sample *A* for various $n_{2\text{DEG}}$. The results of calculations are represented by lines. (a) The results using original Bose-Einstein distribution function. (b) The comparison of the above-mentioned results with those obtained from approximate formula for distribution function (dashed lines) in lower temperature range as indicated by inset in Fig. 5(a).

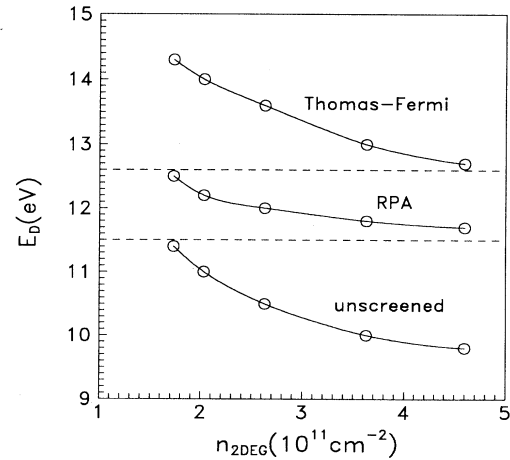


FIG. 6. Deformation potential E_D as a function of 2D electron concentration obtained without screening by 2DEG, with screening in the Thomas-Fermi model and with screening within the framework of the RPA. Lines are to guide the eye (see text).

which overestimates the screening, leads to these values in the high-concentration limit, whereas, neglecting the screening by 2DEG, one gets E_D close to the region mentioned above for low concentrations.

Finally, we would like to check the accuracy of our calculations for the two lowest $n_{2\text{DEG}}$ concentrations, which we rejected at the beginning. The results are given in Fig. 7. We can see that the fits are worse than those in Fig. 5. Also, the values of E_D extracted from these curves (-10.5 and -13.5 eV) differ from the values assumed for the other curves, but they are still reasonable since we estimate that the total error of E_D is about 1 eV.

Considering E_D values as obtained by RPA it seems that the lower values of E_D are more reliable, since they were obtained for higher mobilities (smaller IIS contribution—easier separation of APS). The above effect is demonstrated in Fig. 8, where $1/\mu$ versus $n_{2\text{DEG}}$ is plotted. We can see from this figure that the agreement between calculated and observed mobilities is good for all but the lowest value of $n_{2\text{DEG}}$.

The calculated and experimentally obtained temperature variation of mobility for sample *B* is shown in Fig. 1 of Ref. 10. One can see from that figure that IIS is significant only at helium temperature and between 10 and 70 K APS is the dominant mechanism limiting the 2DEG mobility. The best fit to the experimental results is obtained for $E_D = -11.5 \pm 0.5$ eV, which is in agreement with values of E_D obtained for higher values of $n_{2\text{DEG}}$ for the first heterostructure. As it was already mentioned, these lower values of E_D obtained for high 2DEG concentrations are more reliable than those obtained for lower $n_{2\text{DEG}}$.

Moreover, the RPA approach to the screening effects describes well the experimental results of Harris *et al.*⁴² leading to the value of E_D equal to -12 eV. The same result was obtained in a theoretical paper by Kawamura and Das Sarma²¹ (see also Refs. 8 and 9), where the experimental data of Harris *et al.* were analyzed by an

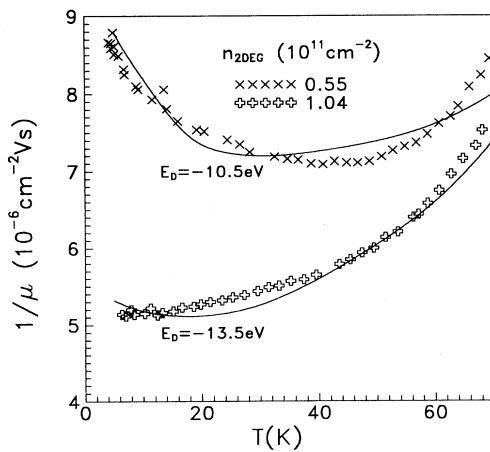


FIG. 7. Reciprocal mobility versus temperature for sample *A* for 2DEG concentrations: $n_{2\text{DEG}} = 0.55$ and $1.04 \times 10^{11} \text{ cm}^{-2}$. The results of calculations are represented by solid lines.

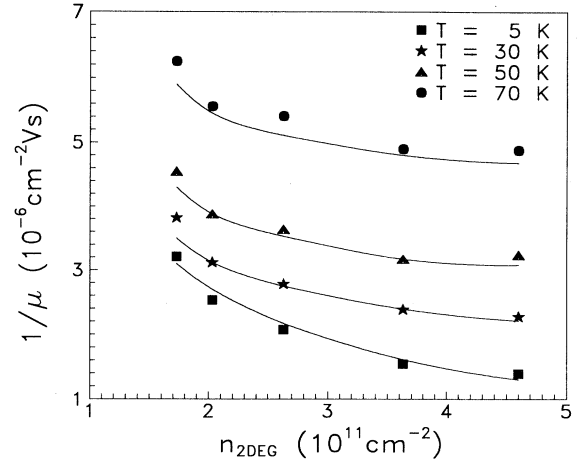


FIG. 8. Reciprocal mobility plotted against the carrier density for different temperatures (sample *A*).

identical screening model, i.e., the RPA approach.

The dependence of $\alpha = 1/\mu_{\text{ac}}T$ on $n_{2\text{DEG}}$ given by Harris *et al.*⁴² in comparison with our experimental and theoretical results for both heterostructures is shown in Fig. 9. Various curves correspond to different models for screening in 2DEG. Our experimental points are defined in the following manner:

$$1/\mu_{\text{ac}}^{\text{exp}} = 1/\mu_{\text{ac}}^{\text{calc}} + (1/\mu_{\text{ac}}^{\text{exp}} - 1/\mu_{\text{ac}}^{\text{calc}}) \quad (19)$$

(i.e., we assume here that the discrepancy between theory and experiment arises mainly from the acoustic phonon contribution). Our results, contrary to those of Refs. 21 and 42, are temperature dependent, so for the above com-

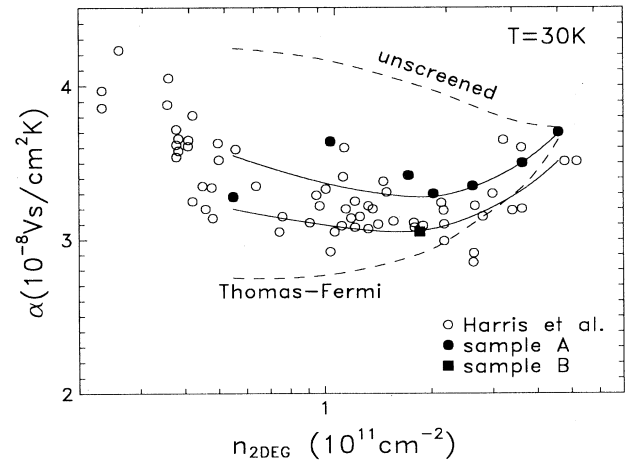


FIG. 9. Reciprocal mobility plotted against carrier density for $T = 30$ K. Theoretical curves correspond to different models for screening in 2DEG and were fitted with E_D values as follows: unscreened, -9.8 eV; RPA and Thomas-Fermi, -12.5 eV.

parison we have taken $T = 30$ K.

Again it follows that only the RPA with E_D between -11.5 and -12.0 eV describes properly both Harris *et al.*⁴² and our experiments. However, other values of E_D were also recently reported and the problem of screening is still discussed. In Table II we collect the most important recent data on the deformation-potential value of GaAs obtained for the GaAs/ $\text{Al}_x\text{Ga}_{1-x}\text{As}$ heterostructure. The reported values are screened by Thomas-Fermi, or RPA, or unscreened by 2DEG. There is only one recent paper in which the authors claim that the screening factor should not be included for the electron-acoustic phonon interaction via the deformation-potential coupling.¹⁹ They obtain $E_D = -8$ eV, concluding that there is no discrepancy between the electron-phonon interactions in the GaAs/ $\text{Al}_x\text{Ga}_{1-x}\text{As}$ heterojunctions and the bulk GaAs. Another unscreened value of $E_D = -9.3$ eV is obtained by Walukiewicz,¹⁸ with the conclusion that a simple Thomas-Fermi screening of the deformation potential cannot be used in the case of 2DEG and a reconsideration of the screening of short-range interactions is needed. In other papers the authors either suggest that the theories of the scattering of 2D electrons by acoustic phonons in GaAs cannot neglect screening^{13-16,20,21} or they present results for both the unscreened and screened cases.¹⁷ The differences in the values of E_D result mainly from the fitting to the different experimental data. We would like to point out that our E_D value is also very close to the one obtained by Hirakawa and Sakaki¹⁶ from a completely different experiment, based on an investigation of the electron heating process in selectively doped GaAs/ $\text{Al}_x\text{Ga}_{1-x}\text{As}$. Due to the discrepancies between the bulk value for E_D and the value measured in heterojunction, there are some suggestions that they may stem from additional scattering mechanisms in heterojunctions, or from the differences in the phonon modes, caused either by the GaAs/ $\text{Al}_x\text{Ga}_{1-x}\text{As}$ interface, or by the proximity of the surface.¹⁷ Concluding, it is still unclear whether the obtained values of E_D are unique to GaAs/ $\text{Al}_x\text{Ga}_{1-x}\text{As}$ heterostructures, or whether they are also more appropriate for bulk GaAs than the traditional value ($E_D \simeq -7$ eV) based on less accurate measurements in bulk material. Note that a similar problem exists for other types of heterostructures, e.g., the value

TABLE II. The absolute values of deformation potentials E_D (in eV) as obtained by different authors.

$ E_D $ (unscreened)	$ E_D $ (screened)		Source
	12 ± 1	(RPA)	Our result
	11.5 ± 12	(RPA)	Ref. 21
	11 ± 13.5	(TF)	Ref. 20
8.0			Ref. 19
9.3			Ref. 18
11.5	16.0	(TF)	Ref. 17
	11 ± 1	(RPA)	Ref. 16
	12.0		Ref. 15
	13.5	(TF)	Ref. 14
	13.5		Ref. 13

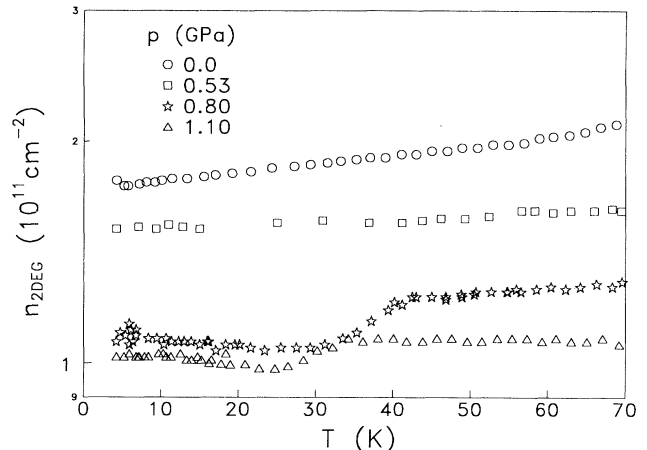


FIG. 10. Experimentally obtained dependence of the 2DEG concentration on temperature for sample B for different values of hydrostatic pressure.

of E_D obtained for Si MOS (metal-oxide semiconductor) is almost twice as large as that derived from electron mobility in bulk Si.⁴³

B. Mobility versus temperature for different values of pressure. Pressure dependence of the deformation potential

The pressure dependence of the electron scattering mechanisms in a specially prepared high-electron-mobility GaAs/ $\text{Al}_x\text{Ga}_{1-x}\text{As}$ heterostructure (sample B) was already described in Ref. 10. To obtain an agreement between theory and experiment we had to assume that the deformation potential (so far treated as pressure independent) depends on pressure. It follows that the absolute value of E_D decreases by about 10%/GPa. One can see from Fig. 3 in Ref. 10 that at higher pressure values (0.8 and 1.1 GPa) and in the temperature range 20–40 K there is a certain disagreement between our theory and the experimental results. In this region of pressure and temperature $n_{2\text{DEG}}$ shows a gradual increase as a function of temperature; as it follows from Fig. 10, the respective change $\Delta n_{2\text{DEG}}$ does not exceed 10% of $n_{2\text{DEG}}$. The inclusion of this effect in our calculations leads to weak changes in the resulting mobility.

V. CONCLUSIONS

In conclusion, we have demonstrated that the proper approach to the electron scattering mechanisms in combination with the experimental method of tuning the 2DEG concentration (in one sample) enables us to obtain good agreement between theoretical and experimental values of mobility in a sample characterized by an unnecessarily extremely high value of μ . In particular, we have determined the value of the conduction-band E_D for GaAs crystal to be about -12.0 eV for one sample and

−11.5 eV for the other. These values are in the range of the most commonly reported values of E_D . We found it interesting that practically the same value (-11 ± 1 eV) was obtained by means of a quite different experimental method—the measurements of the energy-loss rate in 2DEG.¹⁶ This result once more points out the difference in E_D for bulk and 2DEG systems. A good example of even more pronounced differences can be the Si MOS-FET, where the suggested value of E_D is almost twice as large as in bulk Si.³³

The differences mentioned above, as well as some discrepancies between the theoretical results and the experimental data for mobility in the range of temperature where the polar optical phonons scattering plays a significant role, suggest that the interface phonon modes might play some role and should be taken into account. It was proved also that E_D is screened by the 2DEG and for the proper description it is better to use the RPA, which is more general than the Thomas-Fermi approach.

The other result of this work is a finding of the pressure sensitivity of E_D . Its absolute value decreases with increasing pressure by approximately 10%/GPa. The corresponding measurements were performed up to 1.1 GPa. This pressure value also gives the upper limit of our theoretical analysis. We cannot go to higher pressure values for the following reason: The variational wave functions we have used in our calculations may not be sufficiently accurate for small (less than 1) $n_{2\text{DEG}}/n_{\text{depl}}$ ratios²¹ (n_{depl} is the 2D concentration of charge in the depleted region in GaAs and in our case equals about 0.8×10^{12} cm⁻²). At the same time n decreases with pressure—about 40% for

1 GPa—and for pressures higher than 1 GPa it becomes close to n_{depl} .

Two aspects of the problem of the accuracy of dE_D/dp determination can now be discussed. First, uncertainties in the pressure dependencies of the parameters used in the performed fitting procedure (i.e., effective mass, dielectric constant, elastic constants) cause an error of dE_D/dp not exceeding 2%/GPa. Second, there are also effects which are difficult to evaluate properly. For example, we have used the pressure dependence of elastic constants determined for a bulk GaAs sample. Moreover, a certain contribution to the discussed accuracy may originate in effects of 2DEG scattering at the heterostructure interface (interface roughness, interface-phonon scattering). However, we do not expect a significant modification of this contribution after applying pressure. Therefore we point out that the magnitude of dE_D/dp is significant and should not be ignored in examination of pressure effects in heterostructures (as well as in bulk semiconductors where the direct measurements of dE_D/dp are more difficult). This presents an important message for considerations of strained heterostructures consisting of lattice mismatched semiconductors. The internal strain characteristic for these systems can modify E_D significantly.

ACKNOWLEDGMENT

We thank the Polish Committee of Scientific Research for financial support (Grant No. 3 P407 028 07).

- ¹ L. Esaki and R. Tsu (unpublished).
- ² R. Dingle, H. L. Stormer, A. C. Gossard, and W. Wiegmann, *Appl. Phys. Lett.* **33**, 665 (1978).
- ³ T. Saku, Y. Hirayama, and Y. Horikoshi, *Jpn. J. Appl. Phys.* **30**, 902 (1991), and references therein.
- ⁴ E. Litwin-Staszewska, W. Szymanska, and R. Piotrkowski, *Phys. Status Solidi B* **106**, 551 (1981).
- ⁵ R. Piotrkowski, J. L. Robert, E. Litwin-Staszewska, and J. P. Andre, *Phys. Rev. B* **37**, 1031 (1988).
- ⁶ T. Suski, E. Litwin-Staszewska, P. Wisniewski, L. Dmowski, W. H. Zhuang, G. B. Liang, D. Z. Sun, and Y. P. Zen, *J. Appl. Phys.* **63**, 2307 (1988).
- ⁷ L. Konczewicz, E. Litwin-Staszewska, A. Maslowska, R. Piotrkowski, J. L. Robert, and J. P. Andre, *Phys. Status Solidi B* **157**, 593 (1990).
- ⁸ C. Skierbiszewski, I. Gorczyca, E. Litwin-Staszewska, T. Suski, J. Krupski, and K. Ploog, in *Proceedings of the IV International Conference on High Pressure in Semiconductor Physics*, Porto Carras, 1990, edited by D. S. Kyriakos and O. E. Valassiades [Suppl. Sci. Ann. Phys. Dept. Aristotle Univ. 120 (1990)].
- ⁹ I. Gorczyca, C. Skierbiszewski, E. Litwin-Staszewska, T. Suski, J. Krupski, and K. Ploog, *Semicond. Sci. Technol.* **6**, 461 (1991).
- ¹⁰ I. Gorczyca, T. Suski, E. Litwin-Staszewska, L. Dmowski, J. Krupski, and B. Etienne, *Phys. Rev. B* **46**, 4328 (1992).
- ¹¹ E. M. Wolfe, G. E. Stillman, and W. T. Lindley, *J. Appl. Phys.* **41**, 3088 (1970).
- ¹² D. D. Nolte, W. Walukiewicz, and E. E. Haller, *Phys. Rev. Lett.* **59**, 501 (1987).
- ¹³ E. E. Mendez, P. J. Price, and M. Heiblum, *Appl. Phys. Lett.* **45**, 294 (1984).
- ¹⁴ B. J. F. Lin, D. C. Tsui, and G. Weimann, *Solid State Commun.* **56**, 287 (1985).
- ¹⁵ B. Vinter, *Phys. Rev. B* **33**, 5904 (1986).
- ¹⁶ K. Hirakawa and H. Sakaki, *Appl. Phys. Lett.* **49**, 889 (1986).
- ¹⁷ S. J. Manion, M. Artaki, M. A. Emanuel, J. J. Coleman, and K. Hess, *Phys. Rev. B* **35**, 9203 (1987).
- ¹⁸ W. Walukiewicz, *Phys. Rev. B* **37**, 8530 (1988).
- ¹⁹ Y. Okuyama and N. Tokuda, *Phys. Rev. B* **40**, 9744 (1989); **42**, 7078 (1990).
- ²⁰ H. L. Stormer, L. N. Pfeiffer, K. W. Baldwin, and K. W. West, *Phys. Rev. B* **41**, 1278 (1990).
- ²¹ T. Kawamura and Das Sarma, *Phys. Rev. B* **42**, 3725 (1990).
- ²² B. Etienne and E. Paris, *J. Phys. (Paris)* **48**, 2049 (1987).
- ²³ T. Ando, *J. Phys. Soc. Jpn.* **51**, 3900 (1982).
- ²⁴ T. Ando, A. B. Fowler, and F. Stern, *Rev. Mod. Phys.* **54**, 457 (1982).
- ²⁵ F. F. Fang and W. E. Howard, *Phys. Rev. Lett.* **16**, 797 (1966).
- ²⁶ P. J. Price, *Surf. Sci.* **143**, 145 (1984).
- ²⁷ F. Stern, *Phys. Rev. Lett.* **22**, 1469 (1980).

- ²⁸ K. M. Cham and R. G. Wheeler, *Phys. Rev. Lett.* **22**, 1472 (1980).
- ²⁹ P. F. Maldaque, *Surf. Sci.* **73**, 296 (1978).
- ³⁰ F. Stern, *Phys. Rev. Lett.* **18**, 546 (1967).
- ³¹ B. Davydov and I. Shmushkievich, *Zh. Eksp. Teor. Fiz.* **10**, 1044 (1940).
- ³² A. Czachor, A. Holas, S. R. Sharma, and K. S. Singwi, *Phys. Rev. B* **25**, 2144 (1982).
- ³³ K. Hess, *Appl. Phys. Lett.* **35**, 484 (1979).
- ³⁴ B. K. Ridley, *J. Phys. C* **15**, 5899 (1982).
- ³⁵ K. Lee, M. S. Shur, T. J. Drummond, and H. Morkoc, *J. Appl. Phys.* **54**, 6432 (1983).
- ³⁶ B. J. F. Lin, D. C. Tsui, M. A. Paalanen, and A. C. Gosard, *Appl. Phys. Lett.* **45**, 695 (1984).
- ³⁷ P. J. Price, *J. Vac. Sci. Technol.* **19**, 599 (1981).
- ³⁸ F. Abou El-Ela, F. A. Riddoch, M. Davis, and B. K. Ridley, in *Physics of Semiconductors: Proceedings of the 18th International Conference, Stockholm, 1986*, edited by O. Engstrom (World Scientific, Singapore, 1987), p. 1567.
- ³⁹ B. K. Ridley and M. Al-Mudares, *Solid State Electron.* **31**, 683 (1988).
- ⁴⁰ W. Walukiewicz, H. E. Ruda, J. Lagowski, and H. C. Gatos, *Phys. Rev. B* **30**, 4571 (1984).
- ⁴¹ *Semiconductors. Physics of Group IV Elements and III-V Compounds*, edited by O. Madelung, Landolt-Börnstein, New Series, Group III, Vol. 17, Pt. a (Springer, Berlin, 1984).
- ⁴² J. J. Harris, C. T. Foxon, D. Hilton, J. Hewett, C. Roberts, and S. Auzoux, *Surf. Sci.* **229**, 113 (1990).
- ⁴³ S. Kawaji, *J. Phys. Soc. Jpn.* **27**, 906 (1969); see also Y. Shinba and K. Nakamura, *ibid.* **50**, 114 (1981), and references therein.